Contribution from the Research Laboratory of Resources Utilization, Tokyo Institute of Technology, 4259 Nagatsuta, Midori-ku, Yokohama 227, Japan

Dependence of Spectroscopic, Electrochemical, and Excited-State Properties of Tris Chelate Ruthenium(II) Complexes on Ligand Structure

Yuji Kawanishi, Noboru Kitamura, and Shigeo Tazuke*

Received April 19, 1988

Twelve tris chelate ruthenium(II) complexes, RuL_3^{2+}, containing a series of structurally analogous diimine ligands (L) were prepared, and their spectroscopic, redox, and excited-state properties were studied in acetonitrile. Fairly good correlations between the reduction/oxidation potentials of RuL_3^{2+} and the reduction potential/pK_a of L were obtained. Also, the metal-to-ligand charge-transfer (MLCT) absorption/emission energies were explicable in terms of the redox potentials of RuL_3^{2+}. In contrast to the 2,2'-bipyridine (bpy) complex, three RuL_3^{2+} complexes, where L is 6-methyl-4-(2-pyridyl)pyrimidine, 6-phenyl-4-(2-pyridyl)pyrimidine, and 3,3'-bipyridazine, exhibited a small temperature dependence of the emission lifetime, indicating deactivation via thermal activation to the upper lying fourth MLCT excited state. RuL_3^{2+}, where L is 2,2'-bipyrazine or 3,3'-bipyridazine, was superior to $Ru(bpy)_3^{2+}$ in photosensitizing the photoreduction of methylviologen. Synthetic control of efficient photoredox sensitization is possible by modulating ligand properties: the π-accepting and σ-donating abilities of L.

Introduction

A number of tris chelate and mixed-ligand ruthenium(II) complexes have been prepared, and their spectroscopic and electrochemical properties have been targets of active investigation.[1] In most cases, the ligands are confined to 2,2'-bipyridine (bpy), 1,10-phenanthroline (phen), or their methyl, phenyl, and carboxyl derivatives and so forth. Such minor modifications of ligands do not bring about large changes in the redox and excited-state properties of these complexes. In contrast to these complexes, tris chelate ruthenium(II) complexes, RuL_3^{2+}, containing bidiazines,[2] biquinolines,[3] and other ligands (L),[4] exhibit greatly different spectroscopic and redox properties in comparison with those of $Ru(bpy)_3^{2+}$. Nevertheless, the lack of systematic investigations on a series of structurally analogous RuL_3^{2+} complexes impedes further development of Ru(II) photochemistry. With the knowledge of the photophysical and photochemical properties as well as the reactivities of the complexes as functions of ligand structures, efficient electron-transfer sensitizers can be designed. We synthesized 12 RuL_3^{2+} complexes with the series of ligands shown in Figure 1.[5] In particular, the use of (2-pyridyl)pyrimidine derivatives as ligands is informative since (i) (2-pyridyl)pyrimidines act as bi-, tri-, or tetradentate ligands depending on the substituent on the pyrimidine ring,[6] (ii) various substituents can be easily introduced on the pyrimidine ring, and (iii) a 2-pyridyl ring can be introduced on the 2- or 4-position of the pyrimidine ring as shown

2-(2-pyridyl)pyrimidine 4-(2-pyridyl)pyrimidine

so that the effects of structural differences between these two

Scheme I. Synthetic Routes to 2-(2-Pyridyl)pyrimidines

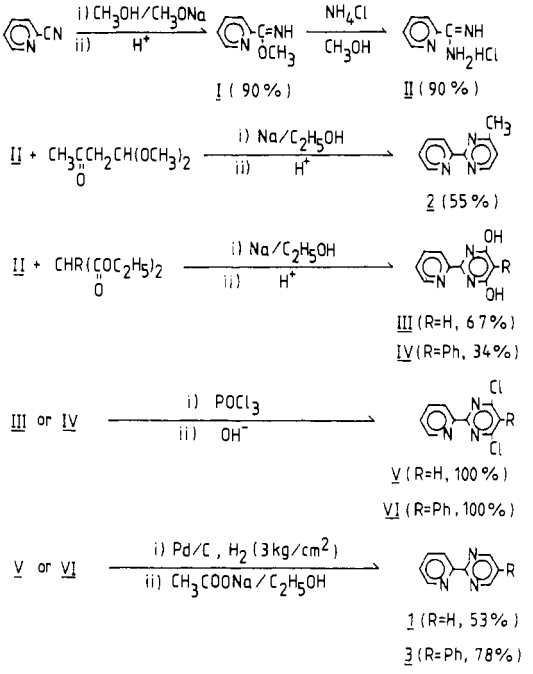

Scheme II. Synthetic Routes to 4-(2-Pyridyl)pyrimidines

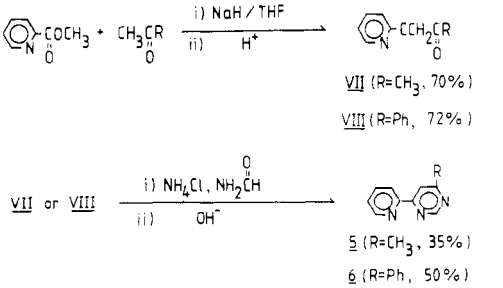

(1) Kalyanasundaram, K. *Coord. Chem. Rev.* **1982**, *46*, 159.

(2) (a) Kitamura, N.; Kawanishi, Y.; Tazuke, S. *Chem. Phys. Lett.* **1983**, *97*, 103. (b) Kawanishi, Y.; Kitamura, N.; Kim, Y.; Tazuke, S. *Sci. Pap. Inst. Phys. Chem. Res. (Jpn.)* **1984**, *78*, 212. (c) Kitamura, N.; Kawanishi, Y.; Tazuke, S. *Chem. Lett.* **1983**, 1185. (d) Tazuke, S.; Kitamura, N. *Pure Appl. Chem.* **1984**, *56*, 1269.

(3) Balzani, V.; Juris, A.; Barigelletti, F.; Belser, P.; von Zelewsky, A. *Sci. Pap. Inst. Phys. Chem. Res. (Jpn.)* **1984**, *78*, 78 and reference cited therein.

(4) (a) Rillema, D. P.; Callahan, R. W.; Mack, K. B. *Inorg. Chem.* **1982**, *21*, 2589. (b) Krug, W. P.; Demas, J. N. *J. Am. Chem. Soc.* **1979**, *101*, 4394. (c) Fuchs, Y.; Lofters, S.; Dieter, T.; Shi, W.; Morgan, R.; Streckas, T. C.; Gafney, H. D.; Baker, A. D. *J. Am. Chem. Soc.* **1987**, *109*, 2691.

(5) Although there are several possible structural isomers for RuL_3^{2+} (L = **1-3**, **5**, **6**), we have not identified the absolute structure. The complexes were analytically pure as judged by elemental analysis and TLC, as well as by cyclic voltammetry. There was no indication of the presence of structural isomers in the present samples.

(6) 4,6-Bis(2-pyridyl)pyrimidine as a tetradentate ligand can be easily prepared according to Scheme II, where R = 2-pyridyl. The corresponding binuclear complex tetrakis(2,2'-bipyridine)[μ-4,6-bis(2-pyridyl)pyrimidine]diruthenium(II) was obtained in a moderate yield (52%) by reacting *cis*-$Ru(bpy)_2Cl_2$ with the ligand. The complex exhibited MLCT absorptions around 430, 531, and 570 nm in acetonitrile but was almost nonemissive at room temperature (Kawanishi, Y.; Kitamura, N.; Tazuke, S. Unpublished results).

0020-1669/89/1328-2968$01.50/0

Table I. Analytical Data for Tris Chelate Ruthenium(II) Complexes[a]

L	formula of RuL_3^{2+}	H_2O[b]	yield,[c] %	anal., % found C	found H	found N	calcd C	calcd H	calcd N
1	$RuC_{27}H_{21}N_9Cl_2$	5	32	44.53	4.55	16.89	44.21	4.26	17.18
2	$RuC_{30}H_{27}N_9Cl_2$	4	56	47.53	4.12	16.47	47.56	4.66	16.44
3	$RuC_{45}H_{33}N_9Cl_2$	3.5	88	58.01	4.48	13.26	57.82	4.31	13.48
4	$RuC_{24}H_{18}N_{12}Cl_2$	5	36	39.12	2.88	22.84	39.14	3.83	22.82
5	$RuC_{30}H_{27}N_9Cl_2$	3	36	48.43	4.11	16.72	48.72	4.50	17.04
6	$RuC_{45}H_{33}N_9Cl_2$	4	51	57.41	4.49	13.27	57.26	4.38	13.36
7	$RuC_{30}H_{30}N_{12}Cl_2$	2	36	46.41	4.29	21.48	45.92	4.62	21.42
8	$RuC_{24}H_{18}N_{12}Cl_2$	3	70	41.32	3.17	23.71	41.15	3.45	23.99
9	$RuC_{24}H_{18}N_{12}Cl_2$	2	54	42.24	2.95	24.57	42.24	3.25	24.63

[a] Analyzed as a chloride salt. [b] The number of hydrated waters. [c] Synthetic yield.

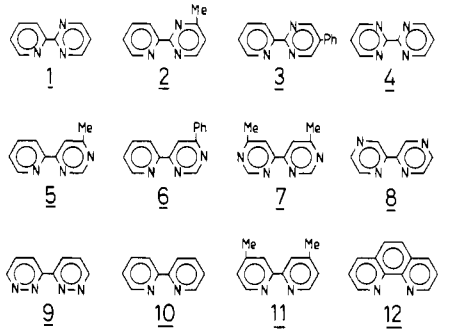

Figure 1. Structures and abbrevations for the diimine ligands (L): **1**, 2-(2-pyridyl)pyrimidine; **2**, 4-methyl-2-(2-pyridyl)pyrimidine; **3**, 5-phenyl-2-(2-pyridyl)pyrimidine; **4**, 2,2′-bipyrimidine; **5**, 6-methyl-4-(2-pyridyl)pyrimidine; **6**, 6-phenyl-4-(2-pyridyl)pyrimidine; **7**, 6,6′-dimethyl-4,4′-bipyrimidine; **8**, 2,2′-bipyrazine; **9**, 3,3′-bipyridazine; **10**, 2,2′-bipyridine; **11**, 4,4′-dimethyl-2,2′-bipyridine; **12**, 1,10-phenanthroline.

isomers on the redox, spectroscopic, and excited-state properties of RuL_3^{2+} can be studied.

In the following, we are presenting an integrated feature of spectroscopic, electrochemical, and excited-state properties of 12 RuL_3^{2+} complexes in acetonitrile. Although a part of the present study has been briefly reported,[2a,b] this detailed discussion of the data for newly prepared RuL_3^{2+} complexes (L = 2-(2-pyridyl)-pyrimidine and 4-(2-pyridyl)pyrimidine derivatives) together with the previous results provides an overall view of the photochemical and photophysical processes of RuL_3^{2+} complexes.

Experimental Section

Synthesis of Diimine Ligands and Their RuL_3^{2+} Complexes. Synthetic routes to 2-(2-pyridyl)pyrimidines and 4-(2-pyridyl)pyrimidines are shown in Schemes I and II, respectively. 2-(2-Pyridyl)pyrimidines were synthesized according to the method of Lafferty and Case,[7] and the yield of each individual process is included in the schemes. The general synthetic procedure for 4-(2-pyridyl)pyrimidines has been reported by Levine and Sneed.[8] The preparation and purification of 2,2′-bipyrimidine (**4**), 6,6′-dimethyl-4,4′-bipyrimidine (**7**) and 2,2′-bipyrazine (**8**), and 3,3′-bipyridazine (**9**) have been reported by Bly and Mellon,[9] Haginiwa et al.,[10] and Lafferty and Case,[7] respectively.

All RuL_3^{2+} complexes were prepared by refluxing dichlorotetrakis-(dimethyl sulfoxide)ruthenium(II)[11] with an excess amount of the desired ligand in an appropriate solvent (typically, ethanol) for several hours. After the solvent was removed under reduced pressure, the resulting solids were washed with benzene to remove the excess ligand and then chromatographed on a Toyopearl HW-40-coarse column (Toyo Soda Co. Ltd.) with ethanol. The yields and analytical data for RuL_3^{2+} (except for $Ru(bpy)_3^{2+}$, $Ru(Me_2\text{-}bpy)_3^{2+}$, and $Ru(phen)_3^{2+}$) are summarized in Table I. Further details of the preparation and purification of both diimine ligands and RuL_3^{2+} have been described elsewhere.[12,13]

Table II. Spectroscopic Properties of RuL_3^{2+} Complexes in Acetonitrile at 298 K[a]

L in RuL_3^{2+}	abs λ_{max}, nm (log ϵ) MLCT[b]	abs λ_{max}, nm (log ϵ) LC[c]	emissn λ_{max}, nm 298 K	emissn λ_{max}, nm 77 K[d]	$10^{-2}\phi^{em}$	τ, ns
1	431 (3.99)	278 (4.65)	633	585	0.096	150
2	451 (4.01)	275 (4.79)	634	594	1.0	290
3	455 (3.98)	303 (4.89)	625	595	1.9	340
4	331 (4.23)	258 (4.70)	634	588	0.49	90
	450 (3.94)					
5	471 (4.10)	281 (4.90)	670	625	1.6	230
6	487 (4.32)	313 (4.89)	676	640	2.6	320
7	497 (4.00)	280 (4.77)	712	662	0.18	40
8	439 (4.14)	291 (4.75)	621	573	2.3	600
9	360 (4.07)	232 (4.54)	652	601	4.4	1050
	412 (4.08)	264 (4.39)				
	447 (4.08)					
10	449 (4.17)	286 (4.94)	620	580	7.0	850
11	458 (4.23)	286 (4.99)	633	593	6.1	830
12	420 (4.19)	262 (5.01)	604	564	2.0	400
	443 (4.22)					

[a] The data reported previously (ref 2b) are slightly different from the present results. Repeated experiments (with improved accuracy of the apparatus) indicate that the present data are more reliable than those in ref 2b. [b] MLCT = metal-to-ligand charge-transfer band. [c] LC = ligand-centered band. [d] In ethanol–methanol (4/1 v/v). Error limits in determining ϕ^{em} and τ are ±10% and ±4%, respectively.

Other Materials. Acetonitrile was refluxed over calcium hydride for several hours and fractionally distilled prior to use. Spectroscopic grade ethanol and methanol (Kanto Chemical Industries) were used as supplied. Tetra-*n*-butylammonium perchlorate as a supporting electrolyte for electrochemical measurements was prepared by metathesis by adding perchloric acid to aqueous tetra-*n*-butylammonium bromide solution and was purified by repeated recrystallizations from a diethyl ether–acetone mixture. Methylviologen (Nakarai Chemicals) and triethanolamine (Kanto Chemical Industries) were used without further purification.

Apparatus and Procedures. Absorption and emission spectroscopy were performed on a Hitachi 320 spectrophotometer and a Hitachi MPF-4 spectrofluorometer, respectively. Emission spectra were corrected by the use of several standard samples as reported by Lippert et al.[14] For the determination of the emission quantum yield of RuL_3^{2+}, the absorbance of a complex at the exciting wavelength (450 nm) was adjusted to 0.05. The emission yield of $Ru(bpy)_3^{2+}$ in water (0.042) was used as the standard,[15] and the refractive index of the solvent (acetonitrile throughout this study unless otherwise stated) was corrected. Emission lifetimes of RuL_3^{2+} at various temperatures were determined by the system reported previously.[16] All the samples for emission spectroscopy were deaerated by argon gas purging over 20 min. The details of the photodecomposition experiments on RuL_3^{2+} in the presence of KSCN as well as of cyclic voltammetry have already been reported.[17]

For photoreduction of methylviologen (MV^{2+}), RuL_3^{2+} was irradiated at 435 nm with a spectroirradiator equipped with a 2-kW xenon lamp (Ushio Electric Co. Ltd.) and a monochromator (JASCO, Model CT-

(7) Lafferty, J. J.; Case, F. H. *J. Org. Chem.* **1967**, *32*, 1591.
(8) Levine, R.; Sneed, J. K. *J. Am. Chem. Soc.* **1951**, *73*, 5614.
(9) Bly, D. B.; Mellon, M. G. *J. Org. Chem.* **1962**, *27*, 2945.
(10) Haginiwa, J.; Higuchi, Y.; Nishioka, K.; Yokokawa, Y. *Yakugaku Zasshi* **1978**, *98*, 67.
(11) Evans, . P.; Spencer, A.; Wilkinson, G. *J. Chem. Soc., Dalton Trans.* **1973**, 204.
(12) Kitamura, N. Ph.D. Thesis, Tokyo Institute of Technology, 1983.
(13) Kawanishi, Y. Ph.D. Thesis, Tokyo Institute of Technology, 1985.
(14) Lippert, E.; Nagele, W.; Seibold-Blankenstein, I.; Staiger, V.; Voss, W. Fresenius' *Z. Anal. Chem.* **1956**, *170*, 1.
(15) Van Houten, V.; Watts, R. J. *J. Am. Chem. Soc.* **1976**, *98*, 4853.
(16) Kitamura, N.; Okano, S.; Tazuke, S. *Chem. Phys. Lett.* **1982**, *90*, 13.
(17) Kitamura, N.; Sato, M.; Kim, H.-B.; Obata, R.; Tazuke, S. *Inorg. Chem.* **1988**, *27*, 651.

Table III. Redox Potentials of the Ligands and RuL_3^{2+} in Acetonitrile at 298 K

L in RuL_3^{2+}	$E_{1/2}$, V vs SCE						
	L/L^-	Ru^{3+}/Ru^{2+}	Ru^{2+}/Ru^+	Ru^+/Ru^0	Ru^0/Ru^-	Ru^{3+}/Ru^{*2+} [a]	Ru^{*2+}/Ru^+ [a]
1	−2.07	+1.44	−1.23	−1.39	−1.58	−0.68	+0.89
2	−2.07	+1.38	−1.18	−1.36	−1.58	−0.71	+0.91
3	−1.89	+1.45	−1.08	−1.24	−1.42	−0.63	+1.00
4	−1.80	+1.69	−0.91			−0.42	+1.20
5	−1.88	+1.38	−1.04	−1.21	−1.42	−0.60	+0.94
6	−1.75	+1.39	−0.97	−1.11	−1.32	−0.55	+0.97
7	−1.54	+1.49	−0.78	−0.91	−1.09	−0.38	+1.09
8	−1.70	+1.86 [b]	−0.80 [b]	−0.98 [b]	−1.24 [b]	−0.30	+1.36
9	−1.84	+1.58	−1.00	−1.25	−1.54	−0.48	+1.06
10	−2.18	+1.27	−1.34	−1.53	−1.78	−0.87	+0.80
11	−2.24	+1.10	−1.45	−1.63		−0.99	+0.64
12	−2.04	+1.27	−1.35	−1.46		−0.93	+0.85

[a] Estimated on the basis of the ground redox potentials and the emission spectra of RuL_3^{2+} at 77 K. [b] Data taken from ref 22.

25C). The incident light intensity was determined by a chemical actinometer. The yields of MV^{2+} photoreduction were calculated on the basis of the absorbance of MV^+ at 603 nm ($\epsilon = 1.17 \times 10^4$ M^{-1} cm^{-1}).[12] All samples were deoxygenated by several freeze–pump–thaw cycles.

Results and Discussion

Absorption and Emission Spectra of RuL_3^{2+}. Absorption and emission spectra of RuL_3^{2+} in acetonitrile at 298 K are shown in Figure 2 together with the emission spectra in ethanol–methanol (4/1 v/v) at 77 K. The spectroscopic data including emission lifetimes (τ) and quantum yields (ϕ^{em}) of RuL_3^{2+} are summarized in Table II.

The present RuL_3^{2+} complex showed intense MLCT (metal-to-ligand charge-transfer) and LC (ligand-centered) transitions around 450–500 nm ($\epsilon = (1–2) \times 10^4$ M^{-1} cm^{-1}) and 250–300 nm ($\epsilon = (5–10) \times 10^4$ M^{-1} cm^{-1}), respectively, similar to those of $Ru(bpy)_3^{2+}$.[1] The assignment of the LC transition was also confirmed by comparing the absorption spectra of the free ligands.

Besides the MLCT absorption around 450 nm, RuL_3^{2+} complexes containing 2-(2-pyridyl)pyrimidines as ligands (L = **1–4**) exhibit relatively strong absorption around 300–350 nm (ϵ = 7000–18 000 M^{-1} cm^{-1}) while the absorption spectra of RuL_3^{2+} complexes with 4-(2-pyridyl)pyrimidines (L = **5–7**) are similar to that of $Ru(bpy)_3^{2+}$ except for their peaking wavelengths (Figure 2). The free 2-(2-pyridyl)pyrimidines (**1–4**) do not have strong absorptions above 300 nm so that the relatively strong absorption of $Ru[2\text{-}(2\text{-pyridyl})pyrimidines]_3^{2+}$ (L = **1–4**) around 300–350 nm is not attributable to a LC transition.

According to Ernst and Kaim,[18] the energy difference between the lowest unoccupied molecular orbital (LUMO) and the second LUMO (SLUMO) of 2,2′-bipyrimidine or 3,3′-bipyridazine is smaller than that of bpy. The relatively strong absorption around 300–350 nm for $Ru[2\text{-}(2\text{-pyridyl})pyrimidines]_3^{2+}$ (L = **1–4**) will be thus attributable to the transition from a $d\pi$ orbital to the SLUMO of L, the second MLCT absorption. The absence of the second MLCT absorption above 300 nm for Ru(6,6′-dimethyl-4,4′-bipyrimidine)$_3^{2+}$ (L = **7**) agrees with the fact that the LUMO–SLUMO gap of 4,4′-bipyrimidine, is the largest among four bidiazines (2,2′-bipyrimidine, 6,6′-dimethyl-4,4′-bipyrimidine, 2,2′-bipyrazine, and 3,3′-bipyridazine).[18] 3,3′-Bipyridazine (**9**), having the smallest LUMO–SLUMO gap, has been reported to exhibit the second MLCT absorption in the visible region for $LM(CO)_4$ (M = Cr, Mo, W).[18] The characteristic absorption bands of Ru(3,3′-bipyridazine)$_3^{2+}$ may be therefore due to the second MLCT transition as well.

In contrast to the characteristic absorption spectra of RuL_3^{2+}, the MLCT emission spectra are almost identical with each other except for their peaking wavelengths in acetonitrile at 298 K as well as in ethanol–methanol (4/1 v/v) at 77 K. The maximum wavelength ranges from 604 nm (Ru(phen)$_3^{2+}$) to 712 nm (Ru(6,6′-dimethyl-4,4′-bipyrimidine)$_3^{2+}$) at 298 K depending on L.

In ethanol–methanol at 77 K, the vibrational structure of the emission spectrum is well resolved. The vibrational progression

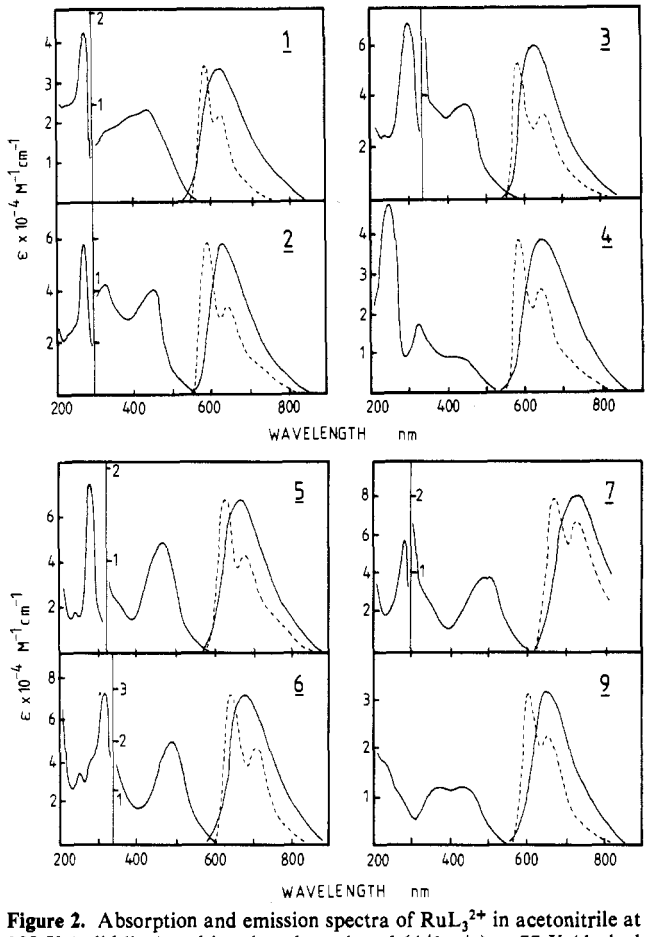

Figure 2. Absorption and emission spectra of RuL_3^{2+} in acetonitrile at 298 K (solid line) and in ethanol–methanol (4/1 v/v) at 77 K (dashed line). The numbering is for RuL_3^{2+}.

($\Delta\nu$) in the spectrum of $Ru(bpy)_3^{2+}$ corresponds to the vibrational stretching of the bpy moiety.[19] $\Delta\nu$ = 1340 cm^{-1} determined for $Ru(bpy)_3^{2+}$ in the present study coincides very well with the reported value (1350 cm^{-1}).[19] For the other RuL_3^{2+} complexes, $\Delta\nu$ values are almost constant at around 1300–1400 cm^{-1} while Ru(3,3′-bipyridazine)$_3^{2+}$ (L = **9**) shows a slightly smaller value of ~1200 cm^{-1}.

Redox Potentials of RuL_3^{2+} Complexes. Redox potentials of L and RuL_3^{2+} in acetonitrile at 298 K are summarized in Table III. The reduction potentials of the free ligands, $E_{1/2}(L/L^-)$, are in general more positive than that of bpy except for Me_2-bpy, indicating that these diimine ligands are better π-acceptors toward a σ-donating metal ion. For bidiazines, the sequence of the LUMO energy 2,2′-bipyrazine (**8**) < 2,2′-bipyrimidine (**4**) < 3,3′-bipyridazine (**9**) < bpy (**10**)[18] is in good agreement with that of the

(18) Ernst, S.; Kaim, W. *J. Am. Chem. Soc.* **1986**, *108*, 3578.

(19) Caspar, J. V.; Meyer, T. J. *J. Am. Chem. Soc.* **1983**, *105*, 5583.

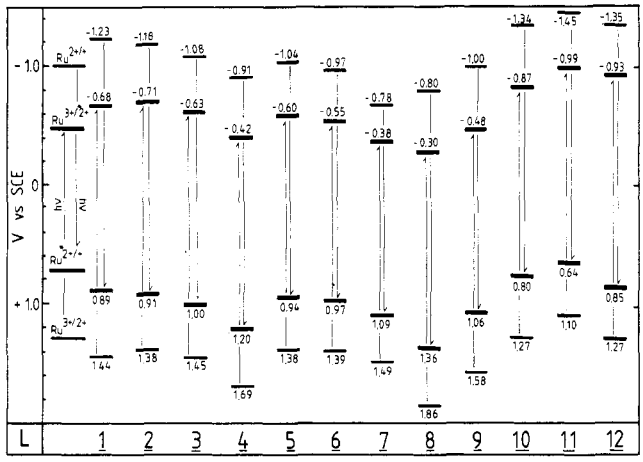

Figure 3. Ground- and excited-state redox potentials of RuL_3^{2+} in acetonitrile at 298 K. The numbering is for RuL_3^{2+}.

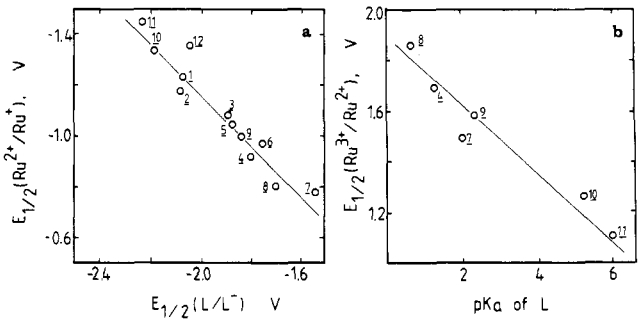

Figure 4. Correlations of the reduction (a) and oxidation (b) potentials of RuL_3^{2+} with the reduction potential and pK_a of L, respectively. pK_a values shown in Figure 5b were determined in water at 293–298 K for pyrimidine (**4**, 1.3), 4-methylpyrimidine (**7**, 2.0), pyrazine (**8**, 0.7), pyridazine (**9**, 2.3), pyridine (**10**, 5.2), and 4-methylpyridine (**11**, 6.0).[21] The numbering is for RuL_3^{2+}.

reduction potential of L, e.g. **8** ($E_{1/2}(L/L^-) = -1.70$ V) > **4** (−1.80 V) > **9** (−1.84 V) > bpy (−2.18 V). The $E_{1/2}(L/L^-)$ value of 6,6′-dimethyl-4,4′-bipyrimidine (**7**) was determined to be −1.54 V, and **7** is the strongest π-accepting ligand among all L groups.

RuL_3^{2+} showed several reversible waves corresponding to successive one-electron oxidation, $E_{1/2}(Ru^{3+}/Ru^{2+})$, and reduction, $E_{1/2}(Ru^{2+}/Ru^+)$, $E_{1/2}(Ru^+/Ru^0)$, and $E_{1/2}(Ru^0/Ru^-)$. For the complexes with bpy, Me_2-bpy, and phen as ligands, the present observations were in good agreement with the reported values.[1,20] The excited-state redox potentials of RuL_3^{2+} were calculated on the basis of the ground-state redox potentials (Table III) and the emission maximum energy of RuL_3^{2+} at 77 K (Table II) as shown in Table III and Figure 3. The present RuL_3^{2+} complexes cover a wide range of reduction ($E_{1/2}(Ru^{3+}/Ru^{*2+}) = +0.64$ to +1.36 V) and oxidation potentials ($E_{1/2}(Ru^{*2+}/Ru^+) = -0.30$ to −0.99 V vs SCE) in the excited state. Efficient photoredox reaction systems are thus expected to be constructed by appropriate choices of RuL_3^{2+} as discussed later.

Implication of the Spectroscopic and Redox Properties of RuL_3^{2+} with Regard to Ligand Structures. Large changes in the spectroscopic and redox properties of RuL_3^{2+} with changes in L are explained on the basis of the σ-donating and/or π-accepting abilities of L. As shown in Figure 4a, an excellent linear relation between $E_{1/2}(Ru^{2+}/Ru^+)$ and $E_{1/2}(L/L^-)$ was obtained with a slope of −1.0, (correlation coefficient (r) −0.96). The slope of unity indicates that the reduction potentials of RuL_3^{2+} are determined by the reduction potentials of L: i.e., the π-acceptor strength of the ligands. On the other hand, the σ-donor strength of L (i.e., the pK_a value of the ligating nitrogen of L) is the main factor modulating the metal d-orbital energies. Weaker σ-donation to a central metal ion results in a higher formal charge of the metal ion and, consequently, the stabilization of the metal d orbitals. Although the available data for pK_a values of L are still limited, a good correlation between the $E_{1/2}(Ru^{3+}/Ru^{2+})$ and pK_a values of L was obtained as shown in Figure 4b (slope −0.124; r = −0.97).[21] It is noteworthy that π-back-bonding of the dπ orbitals to L leads to the stabilization of Ru(II) as well. The π-accepting and σ-donating abilities of L interact synergistically in RuL_3^{2+} through π-back-bonding as discussed in detail by Lever et al.[22] and Rillema et al.[23]

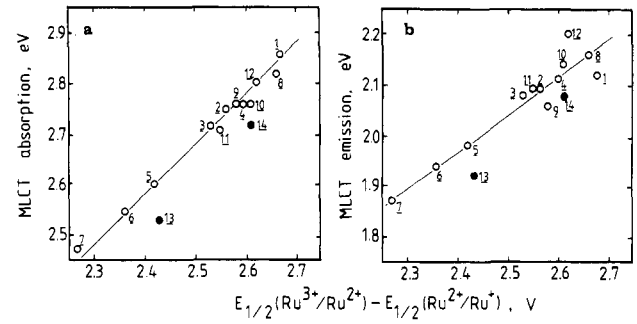

Figure 5. Dependence of the MLCT absorption (a, in acetonitrile at 298 K) and emission energies (b, in ethanol–methanol at 77 K) on the redox potentials of RuL_3^{2+}. The data for $Ru(\mathbf{13})_3^{2+}$ and $Ru(\mathbf{14})_3^{2+}$ are taken from ref 27 and 28, respectively.

The energy difference between the metal t_{2g} (HOMO) and the ligand π^* orbitals (LUMO) should correspond to the MLCT transition energy. Indeed, the MLCT absorption or emission energy of RuL_3^{2+} correlated linearly with $E_{1/2}(Ru^{3+}/Ru^{2+}) - E_{1/2}(Ru^{2+}/Ru^+)$ with a slope of 0.90 (r = 0.98) or 0.73[24] (r = 0.95), respectively (Figure 5).

The relationships analogous to Figures 4 and/or 5 have been reported by Rillema et al.,[23] Ohsawa et al.,[25] and Dodsworth and Lever.[26] All the data are, however, limited to a series of mixed-ligand ruthenium(II) complexes of the type $RuL_nL'_{3-n}^{2+}$, where L and L′ are bpy and its derivatives,[23,25,26] 2,2′-bipyrazine (**8**),[23,25] 2,2′-bipyrimidine (**4**),[23] 2-(2-pyridyl)quinoline,[25] biquinoline derivatives,[26] etc.[26] In contrast to the case for these mixed-ligand complexes, the variation of three ligands in RuL_3^{2+} at once may bring about large changes in the metal–ligand (M–N) bond length and the dihedral angle between ligands. The planarity of a ligand will also be influenced by the introduction of substituents. The linear plots in Figures 4 and 5, however, prove that the π-accepting and σ-donating abilities of L determine the redox and spectroscopic properties of RuL_3^{2+} regardless of the ligand structure.

It is noteworthy that the spectroscopic and redox properties of RuL_3^{2+} containing 3,3′-dicarboethoxy-2,2′-bipyridine (**13**)[27] or 3,3′-dimethyl-2,2′-bipyridine (**14**)[28] ligands do not fall on the lines depicted for the rest of the RuL_3^{2+} complexes (Figure 5).[27] For $Rh(\mathbf{14})_3^{3+}$, the dihedral angle between two pyridine planes of individual **14** ligands was reported to be about 30°,[29] so that the coordination structures of $Ru(\mathbf{13})_3^{2+}$ and $Ru(\mathbf{14})_3^{2+}$ are thought to be different from those of other RuL_3^{2+} complexes. This may be the primary reason for the mismatch of the data for $Ru(\mathbf{13})_3^{2+}$ and $Ru(\mathbf{14})_3^{2+}$ in Figure 5.

(20) Takvoyan, N. E. T.; Hemingway, R. E.; Bard, A. J. *J. Am. Chem. Soc.* **1973**, *95*, 6582.

(21) Sasaki, T. *Chemistry of Heterocyclic Compounds*; Tokyo Kagaku, Dojin: Tokyo, 1972.

(22) Crutchley, R. J.; Lever, A. B. P. *J. Am. Chem. Soc.* **1980**, *102*, 7128; *Inorg. Chem.* **1982**, *21*, 2276.

(23) Rillema, D. P.; Allen, G.; Meyer, T. J. Conrad, D. *Inorg. Chem.* **1983**, *22*, 1617.

(24) The absence of 1:1 correspondence between $E_{1/2}(Ru^{3+}/Ru^{2+}) - E_{1/2}(Ru^{2+}/Ru^+)$ and emission energy is attributable to vibrational distortion between the ground and excited emitting states. See also ref 23.

(25) Ohsawa, Y.; Hanck, K. W.; DeArmond, M. K. *J. Electroanal. Chem. Interfacial Electrochem.* **1984**, *175*, 229.

(26) Dodsworth, E. S.; Lever, A. B. P. *Chem. Phys. Lett.* **1985**, *119*, 61.

(27) Kitamura, N.; Nishi, K.; Tazuke, S. Unpublished results.

(28) Juris, A.; Balzani, V.; Belser, P.; von Zelewsky, A. *Helv. Chim. Acta* **1981**, *64*, 2175.

(29) Nishizawa, M.; Suzuki, T. M.; Watts, R. J.; Ford, P. C. *Inorg. Chem.* **1984**, *23*, 1837 and references cited therein.

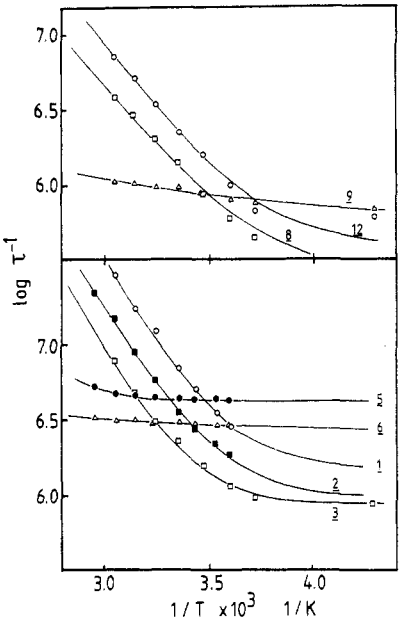

Figure 6. Temperature dependence of the emission lifetime of RuL_3^{2+} in acetonitrile. The numbering is for RuL_3^{2+}.

Table IV. Temperature Dependence of the Emission Lifetimes of RuL_3^{2+} in Acetonitrile

L in RuL_3^{2+}	k', 10^5 s^{-1}	k_r, 10^4 s^{-1}	k_{nr}, 10^6 s^{-1}	ν, s^{-1}	ΔE, cm^{-1}
1	16	0.64	1.6	3.1×10^{14}	3700
2	9.5	3.4	0.92	9.2×10^{13}	3600
3	9.1	5.6	0.85	2.8×10^{14}	3990
4		5.4			
5	44	6.9	4.3	5.2×10^{15}	5270
				$(1.1 \times 10^{7})^a$	$(190)^a$
6	28	8.1	2.7	8.3×10^{7}	1190
				$(5.5 \times 10^{6})^a$	$(120)^a$
7		4.5			
8	2.6	3.8	0.22	5.9×10^{11}	2730
9	6.0	4.2	0.56	3.3×10^{7}	970
				$(3.3 \times 10^{7})^a$	$(250)^a$
10[b]	5.8	7.7	0.48	5.8×10^{13}	3800
11		7.3			
12	4.0	5.0	0.35	2.5×10^{12}	2920

[a] Calculated on the basis of the Arrhenius equation. [b] Data compiled from ref 19. Error limits are as follows: k_r, ±15%; k_{nr}, ±5%; ν, ±20–30%; ΔE, ±100–200 cm^{-1}.

Temperature Dependence of the Emission Lifetime of RuL_3^{2+}. Synthetic control of the emission lifetime (τ) and the emission quantum yield (ϕ^{em}) of RuL_3^{2+} seems to be more difficult than control of the spectroscopic and redox properties. The difficulty arises principally from uncertain decay processes of the excited state, in particular from the complicated temperature dependence.[15,19,23] We studied the temperature dependence of the emission lifetime of RuL_3^{2+} in acetonitrile.

Although the emission lifetimes of all RuL_3^{2+} species decrease with increasing temperature, the temperature dependence of τ is strongly dependent on L as shown in Figure 6. The data in Figure 6 were analyzed by the procedures reported by Meyer and his co-workers (eq 1).[19,30] In eq 1, k_r and k_{nr} are the temperature-independent radiative and nonradiative decay rate constants, respectively. ν and ΔE are the frequency factor and the activation energy for the thermal activation from the lowest emitting MLCT excited state (^{3}MLCT*) to the upper lying, nonemitting d–d excited state (d–d*), respectively.[19,30,31] The results are collected in Table IV.

$$\tau^{-1} = k' + \nu \exp(-\Delta E/RT) = k_r + k_{nr} + \nu \exp(-\Delta E/RT) \quad (1)$$

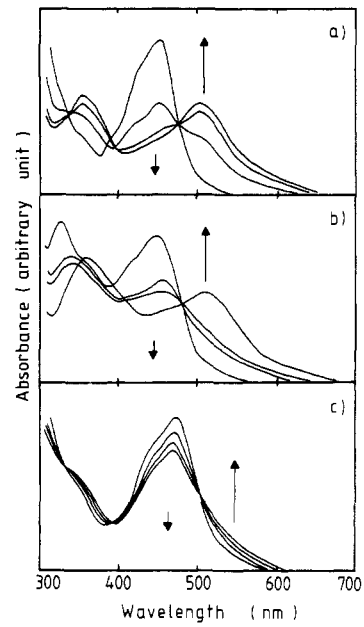

Figure 7. Photochemical reactions of (a) $Ru(bpy)_3^{2+}$ (irradiation time t = 0, 30, 60, and 150 min), (b) Ru[4-methyl-2-(2-pyridyl)pyrimidine]$_3^{2+}$ (L = **2**, t = 0, 5, 10, and 60 min), and (c) Ru[6-methyl-4-(2-pyridyl)-pyrimidine]$_3^{2+}$ (L = **5**, t = 0, 5, 30, 60, and 90 min) with KSCN (0.1 M) in acetonitrile at 298 K.

For RuL_3^{2+} with 2-(2-pyridyl)pyrimidines (**1–3**), 2,2′-bipyrazine (**8**), or phen (**12**) as ligands, τ is strongly dependent on temperature, similar to the lifetime of $Ru(bpy)_3^{2+}$, and the observed ν (10^{12}–10^{14} s^{-1}) and ΔE values (2700–4000 cm^{-1}) are comparable to those reported for $Ru(bpy)_3^{2+}$ ($\nu = 3 \times 10^{12}$–5×10^{13} s^{-1} and ΔE = 3200–3800 cm^{-1}, depending on solvent).[19] The results manifest that the ^{3}MLCT* state of RuL_3^{2+} (L = **1–3, 8, 12**) deactivates through the d–d* state as concluded for $Ru(bpy)_3^{2+}$.[19,30] In marked contrast to these complexes, Ru[6-phenyl-4-(2-pyridyl)pyrimidine]$_3^{2+}$ (L = **6**) and Ru(3,3′-bipyrazine)$_3^{2+}$ (L = **9**) showed a small temperature dependence of τ and ν and ΔE were calculated to be $\sim 10^7$ s^{-1} and 1000–1200 cm^{-1}, respectively. For Ru[6-methyl-4-(2-pyridyl)pyrimidine]$_3^{2+}$ (L = **5**), the computer simulation of the data in Figure 6 by eq 1 gave $\nu = 5.2 \times 10^{15}$ s^{-1} and ΔE = 5270 cm^{-1}. However, as clearly seen in Figure 6, the emission lifetime of $Ru(\mathbf{5})_3^{2+}$ is essentially temeprature independent, similar to that of $Ru(\mathbf{6})_3^{2+}$ or $Ru(\mathbf{9})_3^{2+}$. ν and ΔE values estimated by the Arrhenius equation were 1×10^7 s^{-1} and 190 cm^{-1}, respectively. When one compares ν and ΔE for RuL_3^{2+} (L = **5, 6, 9**) with those for $Ru(bpy)_3^{2+}$, the values for the former complexes are apparently too small to be ascribed to the thermal activation to the d–d* state[32] and, thus, the excited-state decay model involving ^{3}MLCT* and d–d* is not appropriate for RuL_3^{2+} with 4-(2-pyridyl)pyrimidine (**5** or **6**) and 3,3′-bipyridazine (**9**) as ligands.

The participation of the d–d* state in the decay of the excited RuL_3^{2+} can be tested by measuring the photodecomposition of the complex as well. Figure 7 shows the absorption spectra of $Ru(bpy)_3^{2+}$, Ru[4-methyl-2-(2-pyridyl)pyrimidine]$_3^{2+}$ (L = **2**), and Ru[6-methyl-4-(2-pyridyl)pyrimidine]$_3^{2+}$ (L = **5**) in acetonitrile in the presence of 0.1 M KSCN. Upon photoirradiation at 450 nm, $Ru(bpy)_3^{2+}$ and $Ru(\mathbf{2})_3^{2+}$ undergo photoanation with

(30) Durham, B.; Caspar, J. V.; Nagle, J. K.; Meyer, T. J. *J. Am. Chem. Soc.* **1982**, *104*, 4803.

(31) When the ^{3}MLCT* and d–d* states are in equilibrium, ν and ΔE are the rate of ^{3}MLCT* → d–d* conversion and the energy difference between two states, respectively (case I). If the decay of d–d* is very fast, on the other hand, ν and ΔE are the frequency factor and the activation energy relevant to ^{3}MLCT* → d–d* conversion, respectively (case II). ν and ΔE for RuL_3^{2+} (L = **1, 2, 3, 8,** and **12**) are reasonably explained by the case II mechanism. See also ref 19 and 30.

(32) Both ΔE and ν are extremely small as compared with those reported for the case I or II mechanism.[19,30]

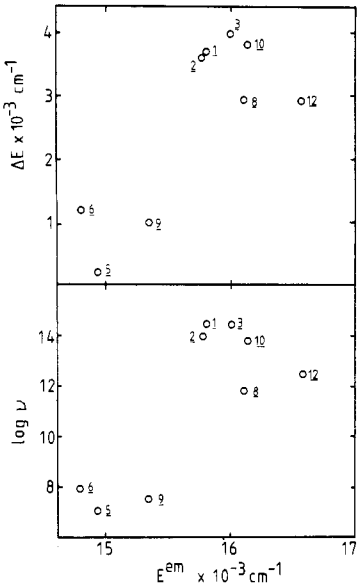

Figure 8. Correlations of ΔE and ν with the emission energy of RuL_3^{2+} (E^{em}). The numbering is for RuL_3^{2+}.

KSCN (and/or CH_3CN) as judged from the changes in the absorption spectra, exhibiting isosbestic points at 474 and 477 nm, respectively. Although we have not identified the product(s) of the photoreaction, the new band that appears around 510 nm is ascribed to a complex of the type $RuL_2(NCS)_2$ or $RuL_2(CH_3CN)(NCS)$.[33] According to Meyer and his co-workers, photoanation of $Ru(bpy)_3^{2+}$ takes place via the d–d* state,[19,30,33] so that the efficient photodecomposition of Ru[4-methyl-2-(2-pyridyl)-pyrimidine]$_3^{2+}$ comparable to that of $Ru(bpy)_3^{2+}$ could be attributed to the participation of the d–d* state in the excited-state decay of the complex. This conclusion agrees very well with the large temperature dependence of τ; $\nu = 9 \times 10^{13}$ s^{-1} and ΔE = 3600 cm^{-1}. On the other hand, the relatively small ν ($(1-8) \times 10^7$ s^{-1}) and ΔE values (200–1200 cm^{-1}) of RuL_3^{2+} (L = 6-methyl-4-(2-pyridyl)pyrimidine (**5**), 6-phenyl-4-(2-pyridyl)pyrimidine (**6**), and 3,3′-bipyridazine (**9**)) reveal that the d–d* state does not participate in the MLCT excited-state decay of these complexes. This interpretation is in accordance with the higher stabilities of these complexes against photoreaction. The yields of the photodecomposition for RuL_3^{2+} (L = **5**, **6**, **9**) were only ~20% of that for $Ru(bpy)_3^{2+}$ or Ru[4-methyl-2-(2-pyridyl)pyrimidine]$_3^{2+}$ (L = **2**).

Besides these three complexes, only six Ru(II) complexes have been reported to exhibit the small temperature dependence of τ; $\nu = 4 \times 10^6$–3×10^7 and ΔE = 300–800 cm^{-1}. The complexes are $RuL_nL'_{3-n}$, where L and L′ are bpy, 2,2′-bipyrimidine, 2,2′-bipyrazine, 4,4′-Me_2-2,2′-bpy, 4,4′-$(HO_2C)_2$-bpy, 4,4′-$(EtO_2C)_2$-bpy, and CN^- and the solvents studied are propylene carbonate, dichloromethane, and water.[16,34-36] Small ν (8×10^6 s^{-1}) and ΔE (360 cm^{-1}) values were also observed for Ru(3,3′-bipyridazine)$_3^{2+}$ (L = **9**) in water.[37]

Among the properties of RuL_3^{2+}, the only factor determining the temperature dependence of τ seems to be the energy of the ^{3}MLCT* state. Figure 8 reveals that RuL_3^{2+} species exhibiting a small temperature dependence of τ (L = 6-methyl-4-(2-pyridyl)pyrimidine (**5**), 6-phenyl-4-(2-pyridyl)pyrimidine (**6**), 3,3′-bipyridazine (**9**)) possess relatively low-energy MLCT excited states as compared with those showing a large temperature dependence of τ; $\nu = 10^{12}$–10^{14} s^{-1} and ΔE = 3000–4000 cm^{-1}. This relation is also applicable to the $RuL_nL'_{3-n}$ complexes mentioned above. The emission energies of these complexes at room temperature were all in the range of (14.1–15.2) $\times 10^3$ cm^{-1},[34-36] which are considerably lower relative to that of $Ru(bpy)_3^{2+}$ (16.1×10^3 cm^{-1} in acetonitrile at 298 K).

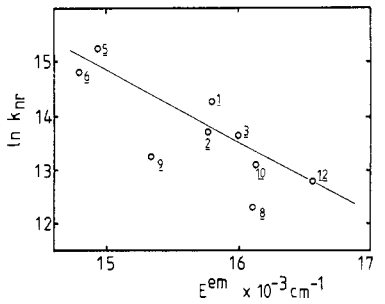

Figure 9. ln k_{nr} vs E^{em} plot for RuL_3^{2+} in acetonitrile. The numbering is for RuL_3^{2+}.

Provided that the energy of the d–d* state remains almost constant for a series of RuL_3^{2+} complexes,[38] the energy difference between the emitting ^{3}MLCT* state and the nonemitting d–d* state ($\Delta E(^3\text{MLCT*}\text{–}(\text{d–d*}))$) becomes larger when the energy of the ^{3}MLCT* state is lowered. Since $\Delta E(^3\text{MLCT*}\text{–}(\text{d–d*}))$ for $Ru(bpy)_3^{2+}$ has been reported to be ~3600 cm^{-1},[15] those values for Ru[6-methyl-4-(2-pyridyl)pyrimidine]$_3^{2+}$ (L = **5**), Ru[6-phenyl-4-(2-pyridyl)pyrimidine]$_3^{2+}$ (L = **6**), and Ru(3,3′-bipyridazine)$_3^{2+}$ (L = **9**) will be as large as 4400–4900 cm^{-1} as estimated from the emission energies at 298 K (Table II).[39] The thermal activation to the d–d* state is impossible for these complexes. Instead, we suppose that the ^{3}MLCT* state deactivates through the fourth MLCT excited state, MLCT′. For $Ru(bpy)_3^{2+}$, the existence of MLCT′ has been predicted theoretically to be located 600–1000 cm^{-1} above ^{3}MLCT*.[40] For $RuL_nL'_{3-n}$, the small temperature dependence of τ was interpreted by assuming the participation of MLCT′ in the decay of the ^{3}MLCT* state.[35]

Nonradiative Decay of RuL_3^{2+}. Another important factor governing the emission lifetime of RuL_3^{2+} is the nonradiative decay constant (k_{nr}), which is much larger (~10^2) than the radiative decay constant (k_r in Table IV). If the vibrational overlap between the ground and excited states (e.g., Franck–Condon factor) determines k_{nr}, ln k_{nr} should be linearly correlated with E^{em} as predicted by the energy gap law.[19,41] Applicability of the energy gap law was tested as shown in Figure 9.

The electronic interactions between a metal ion and ligands (β_0) should be constant in a series of complexes for the energy gap law to be applicable to k_{nr}.[19,41] The variation of three ligands in RuL_3^{2+} at once will alter the coordination environment so that β_0 might be affected. Nevertheless, the energy gap law can be satisfactorily applied to the present systems as well with a cor-

(33) Durham, B.; Walsh, J. L.; Carter, C. L.; Meyer, T. J. *Inorg. Chem.* **1980**, *19*, 860.
(34) Allen, G. H.; White, R. P.; Rillema, D. P.; Meyer, T. J. *J. Am. Chem. Soc.* **1984**, *106*, 2613.
(35) Wacholtz, W. F.; Auerbach, R. A.; Schmehl, R. H. *Inorg. Chem.* **1986**, *25*, 227.
(36) Henderson, L. J., Jr.; Cherry, W. R. *J. Photochem.* **1985**, *28*, 143.
(37) Kitamura, N.; Kawanishi, Y.; Tazuke, S. Unpublished results.
(38) This assumption is not necessarily correct for a series of RuL_3^{2+} complexes as suggested by the linear correlation of $E_{1/2}(Ru^{3+}/Ru^{2+})$ with the pK_a of L (Figure 4). However, it is also valid that the π-accepting and σ-donating abilities of L in RuL_3^{2+} interact synergistically in RuL_3^{2+} through π-back-donation. Indeed, for example, the weaker σ-donating ability of 2,2′-bipyrazine (**8**) is compensated by the relatively strong π-accepting power of L, giving rise to the MLCT absorption and emission energies of the complex comparable to those of $Ru(bpy)_3^{2+}$. Allen et al. have reported that the variation of ligand structure induces a larger change in the energy of ^{3}MLCT* as compared with that in the d–d* state via donation from L to Ru(III).[34] In the present discussion, we assume that the d–d* state is almost constant in energy with the variation of L relative to the energy of ^{3}MLCT*.
(39) The extremely large ΔE = 5300 cm^{-1} for RuL_3^{2+} (L = **5**) calculated from the computer simulation of the data in Figure 6 may be the actual energy gap or activation energy for the (^{3}MLCT* → d–d*) conversion. In the high-temperature region, τ seems to increase greatly with increasing temperature. If this is the case, $\Delta E(^3\text{MLCT*}\text{–}(\text{d–d*}))$ of RuL_3^{2+} (L = **5**) is very large (~5300 cm^{-1}) as compared with that of $Ru(bpy)_3^{2+}$.
(40) (a) Kober, E. M.; Meyer, T. J. *Inorg. Chem.* **1984**, *23*, 3877. (b) Meyer, T. J. *Pure Appl. Chem.* **1986**, *58*, 1193.
(41) (a) Caspar, J. V.; Kober, E. M.; Sullivan, B. P.; Meyer, T. J. *J. Am. Chem. Soc.* **1982**, *104*, 630. (b) Caspar, J. V.; Sullivan, B. P.; Kober, M. K.; Meyer, T. J. *Chem. Phys. Lett.* **1982**, *91*, 91. (c) Caspar, J. V.; Meyer, T. J. *Inorg. Chem.* **1983**, *22*, 2444. (d) Caspar, J. V.; Meyer, T. J. *J. Phys. Chem.* **1983**, *87*, 952.

relation coefficient of −0.94. Ru(2,2′-bipyrazine)$_3^{2+}$ (L = **8**) and Ru(3,3′-bipyrazine)$_3^{2+}$ (L = **9**) are exceptional (see later discussion). The observed slope of -1.3×10^{-3} cm is also comparable to the reported value.[19,34] The present results indicate that β_0 is relatively insensitive to ligand modification. Thus, the nonradiative decay of RuL$_3^{2+}$ is predictable in terms of the ligand structure determining the E^{em}, $E_{1/2}(L/L^-)$, and pK_a values of L.

The high-frequency acceptor vibration(s) of ligands ($\hbar\omega_M$) determines the slope of a ln k_{nr} vs E^{em} plot (slope = $-\gamma_0/\hbar\omega_M$ and $\gamma_0 = \ln [E^{em}(0\text{–}0)/\hbar\omega_M S_M] - 1$, where $E^{em}(0\text{–}0)$ and S_M are the energy of the 0–0 emission band and the parameter of the excited-state distortion in the acceptor vibration, respectively).[19,41] In spite of the anticipated structural fluctuation of complexes, the vibrational progressions determined by the data in Figure 2 are almost constant at $\Delta\nu$ = 1300–1400 cm^{-1} for all RuL$_3^{2+}$ complexes. This finding is in support of the applicability of the energy gap law. The Franck–Condon analyses of low-temperature emission spectra of RuL$_3^{2+}$ also reached an analogous conclusion.[42] Although the π-accepting and σ-donating capabilities of L are greatly influenced by ligand structures as discussed in the previous sections, the vibrational modes (ν(C–C), ν(C–N), and/or ν(C–H)) do not change appreciably with L.

The large deviation of the data for Ru(2,2′-bipyrazine)$_3^{2+}$ (L = **8**) and Ru(3,3′-bipyridazine)$_3^{2+}$ (L = **9**) from the linear plot can be ascribed to the change in β_0 and/or vibrational modes of L ($\Delta\nu$) for these two complexes. In the case of Ru(3,3′-bipyridazine)$_3^{2+}$, $\Delta\nu$ was estimated to be 1200 cm^{-1} (Figure 2), which is slightly smaller than those for other complexes. However, $-\gamma_0/\hbar\omega_M$ values for Ru(**8**)$_3^{2+}$ and Ru(**9**)$_3^{2+}$ were calculated to be -1.3×10^{-3} and -1.2×10^{-3} cm, respectively, while those for other RuL$_3^{2+}$ complexes were (−0.9 to −1.3) $\times 10^{-3}$ cm.[42,43] The variation of $\hbar\omega_M$ with L will not account for the data of RuL$_3^{2+}$ (L = **8**, **9**). The analogous deviation of ln k_{nr} for a series of Ru(bpy)$_n$(2,2′-bipyrazine)$_{3-n}$ complexes from the linear plot for Ru(bpy)$_n$(2,2′-bipyrimidine)$_{3-n}$ has also been reported by Allen et al.[34] They showed that β_0 for Ru(bpy)$_n$(2,2′-bipyrimidine)$_{3-n}$ was larger than that for Ru(bpy)$_n$(2,2′-bipyrazine)$_{3-n}$. In spite of the structural resemblance between the present diimine ligands, the electronic interaction of 2,2′-bipyrazine or 3,3′-bipyridazine with a central Ru(II) ion is different from those for other RuL$_3^{2+}$ species. Further theoretical and experimental studies are necessary to fully understand the ligand effects on β_0.

RuL$_3^{2+}$ Complexes with 2-(2-Pyridyl)pyrimidines and 4-(2-Pyridyl)pyrimidines as Ligands. It is interesting to compare the redox and spectroscopic properties of RuL$_3^{2+}$ containing the isomers 2-(2-pyridyl)pyrimidines and 4-(2-pyridyl)pyrimidines as ligands. Among RuL$_3^{2+}$ complexes with the structurally analogous ligands **1**–**7**, both redox and spectroscopic properties are strongly dependent on the position of the 2-pyridyl or 2-/4-pyrimidine substituent on the pyrimidine ring. For example, Ru[2-(2-pyridyl)pyrimidines]$_3^{2+}$ (L = **1**–**4**) exhibit a shorter wavelength MLCT absorption (432–455 nm) and emission (625–634 nm) as compared with RuL$_3^{2+}$ species possessing 4-(2-pyridyl)pyrimidines as ligands, **5**–**7** (E^{abs} = 471–497 nm and E^{em} = 670–712 nm). As discussed in the previous section, the π-accepting and σ-donating abilities of L determine these properties. $E_{1/2}(L/L^-)$ values for 2-(2-pyridyl)pyrimidines and 4-(2-pyridyl)pyrimidines are −1.80 to −2.07 and −1.54 to −1.88 V, respectively. Clearly, the π-accepting abilities of 4-(2-pyridyl)-pyrimidines are stronger than those of 2-(2-pyridyl)pyrimidines.

While the σ-donating power of 4-(2-pyridyl)pyrimidines is supposed to be higher than that of 2-(2-pyridyl)pyrimidines as judged from the available data of 2-aminopyridine (pK_a = 3.5) and 4-aminopyrimidine (5.7),[21] the oxidation potentials of Ru[4-methyl-2-(2-pyridyl)pyrimidine]$_3^{2+}$ (L = **2**) and Ru[6-methyl-4-(2-pyridyl)pyrimidine]$_3^{2+}$ (L = **5**) are both 1.38 V, suggesting that the σ-donor strengths of **2** and **5** are comparable. Consequently, the π-accepting strength seems to play a major role in the difference between 2-(2-pyridyl)pyrimidines and 4-(2-pyridyl)pyrimidines. Thus, the LUMO energies of 4-(2-pyridyl)pyrimidines being lower than those of 2-(2-pyridyl)pyrimidines would result in the lower energy MLCT absorption and emission.

The most dramatic difference between two isomers is found in the emission lifetimes of their complexes. Ru[4-(2-pyridyl)-pyrimidines]$_3^{2+}$ (L = **5** and **6**) show a small temperature dependence of τ while Ru[2-(2-pyridyl)pyrimidines]$_3^{2+}$ (L = **1**–**4**) exhibit behavior similar to that of Ru(bpy)$_3^{2+}$ as described in the previous section. Ru[4-(2-pyridyl)pyrimidines]$_3^{2+}$ have larger $\Delta E(^3$MLCT*–(d–d*)) values than Ru[2-(2-pyridyl)pyrimidines]$_3^{2+}$ (Figure 8). Since $\Delta E(^3$MLCT*–(d–d*)) is determined by $E_{1/2}(L/L^-)$, the temperature dependence of τ may be controlled by the fine tuning of ligand structure as well. The large ΔE-(^{3}MLCT*–(d–d*)) value of Ru[6-methyl-4-(2-pyridyl)pyrimidine]$_3^{2+}$ (L = **5**) or Ru[6-phenyl-4-(2-pyridyl)pyrimidine]$_3^{2+}$ (L = **6**), however, accompanies the lower energy MLCT excited state (Figure 8), which inevitably leads to an increase in k_{nr} as predicted by the energy gap law (Figure 9). Indeed, the emission lifetimes of these complexes were 230–320 ns in acetonitrile at 298 K (Table II), which are considerably shorter than that of Ru(bpy)$_3^{2+}$ (850 ns). The emission lifetimes of Ru[2-(2-pyridyl)pyrimidines]$_3^{2+}$ (L = **2** and **3**) and Ru[4-(2-pyridyl)pyrimidines]$_3^{2+}$ (L = **5** and **6**) are nearly identical at τ = 230–340 ns at 298 K. The complexes with small temperature dependences of τ (i.e., Ru[4-(2-pyridyl)pyrimidines]$_3^{2+}$) are obviously more advantageous than Ru[2-(2-pyridyl)pyrimidines]$_3^{2+}$ as photosensitizers.

Photoreduction of Methylviologen by RuL$_3^{2+}$. The actual photoredox abilities of a series of RuL$_3^{2+}$ complexes were estimated by the quantum yield of RuL$_3^{2+}$-sensitized photoreduction of methylviologen (MV^{2+}) in the presence of triethanolamine (TEA) in acetonitrile (Table V). ϕ_{MV^+} represents the quantum yield of MV^+ formation determined from the initial slope of a time-conversion profile, and Q_e is the quenching efficiency defined as $Q_e = 1 - I/I^0$, where I and I^0 are the emission intensities of RuL$_3^{2+}$ in the presence and absence of 5 mM of MV^{2+} or 0.15 M of TEA, respectively. As clearly seen in Table V, ϕ_{MV^+} is dependent on RuL$_3^{2+}$ and a comparable or better quantum yield relative to that sensitized by Ru(bpy)$_3^{2+}$ is obtained with RuL$_3^{2+}$ (L = **3**, **6**, **8**,

Table V. Photoreduction of Methylviologen by RuL$_3^{2+}$ in Acetonitrile[a]

L in RuL$_3^{2+}$	Q_e (ΔG, kcal/mol)[b]		ϕ_{MV^+}	ϕ_{redox}[c]	quenching mechanism
	MV^{2+}	TEA			
1	0.11 (−5.5)	0 (+0.2)	0.031	0.28	II
2	0.25 (−6.2)	0 (−0.2)	0.089	0.36	II
3	0.26 (−4.4)	0.14 (−2.3)	0.29	0.73	I + II
4					
5	0.18 (−3.7)	0.16 (−0.9)	0.16	0.47	I + II
6	0.34 (−2.5)	0.18 (−1.6)	0.26	0.50	I + II
7					
8	0 (+3.2)	1.00 (−10.6)	1.7	1.7	I
9	0.14 (−0.9)	0.40 (−3.7)	0.42	0.78	I + II
10	0.75 (−9.9)	0 (+2.3)	0.33	0.44	II
11					
12	0.62 (−11.3)	0 (+1.2)	0.25	0.40	II

[a] Determined in the presence of 0.15 M of TEA under deaerated conditions. [b] Free energy change of the quenching. $\Delta G(MV^{2+}) = E_{1/2}(Ru^{3+}/{}^*Ru^{2+}) - E_{1/2}(MV^{2+}/MV^+)$. $\Delta G(TEA) = E_{1/2}(TEA^{ox}/TEA) - E_{1/2}({}^*Ru^{2+}/Ru^+)$. $E_{1/2}(MV^{2+}/MV^+)$ and $E_{1/2}(TEA^{ox}/TEA)$ are −0.44 and 0.90 V (vs SCE), respectively. [c] $\phi_{redox} = \phi_{MV^+}/Q_e$. Error limits in determining ϕ_{MV^+} and ϕ_{redox} are ±5%.

(42) Franck–Condon analyses of the emission spectra of RuL$_3^{2+}$ at 77 K were performed by the procedures reported by Caspar et al. (Caspar, J. V.; Westmoreland, T. D.; Allen, G. H.; Bradley, P. G.; Meyer, T. J.; Woodruff, W. H. *J. Am. Chem. Soc.* **1984**, *106*, 3492). On the assumption of $\nu_M = \nu_L = 6$ and $\hbar\omega_L$ = 400 cm^{-1}, the observed emission spectra were simulated by varying five parameters: $\hbar\omega_M$, S_M, S_L, $\Delta\nu_{1/2}$, and $E^{em}(0\text{–}0)$ (for the abbrevations for the parameters, see the reference described above). For RuL$_3^{2+}$ (L = **2**–**6**, **10**–**12**), the best fits of the observed spectra were obtained with $\hbar\omega_M$ = 1400–1450 cm^{-1}, S_M = 0.85–1.15 (= 0.65 for Ru(phen)$_3^{2+}$), S_L = 1.0–1.1, $\Delta\nu_{1/2}$ = 550–700 cm^{-1}, and $E^{em}(0\text{–}0)$ = 15 800–17 900 cm^{-1} (Kim, H.-B.; Kitamura, N.; Tazuke, S. Manuscript in preparation).

(43) $-\gamma_0/\hbar\omega_M$ was calculated on the basis of the best-fit parameters of the emission spectrum. The following values were used for Ru(2,2′-bipyrazine)$_3^{2+}$ (Ru(3,3′-bipyridazine)$_3^{2+}$): $E^{em}(0\text{–}0)$ = 17 600 cm^{-1} (16 750), $\hbar\omega_M$ = 1350 cm^{-1} (1250), and S_M = 0.80 (1.05).

9) as a photosensitizer. As briefly reported,[2c] the photoreaction proceeding via reductive quenching (mechanism I) gives a higher quantum yield as compared with that initiated by oxidative quenching of the excited RuL_3^{2+} by MV^{2+} (mechanism II), in which the unfavorable back electron transfer from MV^+ to RuL_3^{3+} reduces the overall quantum yield. Data in Table V are in good support for the present argument. Namely, the high quantum yields were attained only when mechanism I prevails.

mechanism I (reductive quenching):

$$*RuL_3^{2+} + TEA \rightarrow RuL_3^{+} + TEA^{ox} \not\leftarrow RuL_3^{2+} + TEA$$

$$RuL_3^{+} + MV^{2+} \rightarrow RuL_3^{2+} + MV^{+}$$

mechanism II (oxidative quenching):

$$*RuL_3^{2+} + MV^{2+} \rightarrow RuL_3^{3+} + MV^{+} \rightarrow RuL_3^{2+} + MV^{2+}$$

$$RuL_3^{3+} + TEA \rightarrow RuL_3^{2+} + TEA^{ox}$$

For Ru(2,2′-bipyrazine)$_3^{2+}$ (L = **8**), the quantum yield of 1.7 needs to be explained. In an alkaline medium or at a high TEA concentration as in the present case, the TEA cation radical produced by electron transfer is known to release a proton[44] and the resulting TEA radical is able to reduce another MV^{2+}. In a high-pH region, the overall reaction can be thus expressed as eq 6. Analogous features are observed for Ru(2,2′-bipyrimidine)$_3^{2+}$ in aqueous solution as well ([Ru(2,2′-bipyrimidine)$_3^{2+}$] = 6×10^{-5} M, [MV^{2+}] = 0.02 M, [TEA] = 0.5–1.2 M).[12] In this case, ϕ_{MV^+} increases with the increase in [TEA] and the limiting ϕ_{MV^+} at infinite TEA concentration was 1.56. In a high pH region or at a high TEA concentration, participation of the reactions in eq 4 and 5 cannot be eliminated for all reaction systems examined in this study.

$$*RuL_3^{2+} + TEA \rightarrow RuL_3^{+} + TEA^{ox}(R_2N^{\cdot+}CH_2CH_2OH) \quad (2)$$

$$RuL_3^{+} + MV^{2+} \rightarrow RuL_3^{2+} + MV^{+} \quad (3)$$

$$R_2N^{\cdot+}CH_2CH_2OH \rightleftharpoons R_2NCH_2\dot{C}HOH + H^+ \quad (4)$$

$$R_2NCH_2\dot{C}HOH + MV^{2+} \rightarrow R_2NCH_2CHO + MV^{+} + H^+ \quad (5)$$

$$\text{net: } RuL_3^{2+} + 2MV^{2+} \xrightarrow[TEA]{h\nu} RuL_3^{2+} + 2MV^{+} \quad (6)$$

(44) Kalyanasundaram, K.; Kiwi, J.; Graetzel, M. *Helv. Chim. Acta* **1978**, *61*, 2720.

Conclusions

To develop efficient redox photosensitizers, it is obvious that Ru(bpy)$_3^{2+}$ is not the best among its analogues. On the basis of the present study, modulation of the π-accepting ($E_{1/2}(L/L^-)$) and σ-donating abilities (pK_a) of L is a plausible approach for efficient photoredox systems. For photoreduction of MV^{2+} in the RuL_3^{2+}–MV^{2+}–TEA systems, RuL_3^{2+} complexes having a ground-state reduction potential more positive than −1.2 V are subjected to reductive quenching by TEA and will act as more efficient photosensitizers than Ru(bpy)$_3^{2+}$.

RuL_3^{2+} species (L = **5**, **6**, **9**) possessing a lower ^{3}MLCT* state energy relative to that of Ru(bpy)$_3^{2+}$ showed a smaller temperature dependence of τ (<1000 cm^{-1}). The lowering of the emitting ^{3}MLCT* state energy, however, leads in general to a decrease in the excited-state lifetime (i.e., energy gap law). Among 12 RuL_3^{2+} complexes, only Ru(3,3′-bipyridazine)$_3^2$ (L = **9**) exhibits a small temperature dependence of τ as well as a relatively long emission lifetime (1050 ns at 298 K). Also, this complex shows strong reduction and oxidation abilities and an absorption energy comparable with that of Ru(bpy)$_3^{2+}$. Ru(3,3′-bipyridazine)$_3^{2+}$ certainly has more advantages than Ru(bpy)$_3^{2+}$ as a photoredox sensitizer.

Acknowledgment. We are greatly indebted to H.-B. Kim and M. Sato for their collaboration in lifetime measurements and photodecomposition experiments, respectively. This work was partly supported by a Grant-in-Aid for Special Study from the Ministry of Education, Science and Culture of Japan (No. 61040046).

Contribution from the University Chemical Laboratory, University of Cambridge, Lensfield Road, Cambridge CB2 1EW, England

Intensity Distributions within the "d–d" Spectra of Tetrakis(diphenylmethylarsine oxide)(nitrato)cobalt(II) and Tetrakis(diphenylmethylarsine oxide)(nitrato)nickel(II) Nitrates†

Neil D. Fenton and Malcolm Gerloch*

Received August 4, 1988

The relative intensities of the polarized "d–d" transitions of the title complexes have been reproduced quantitatively within a new ligand-field scheme. The model is parametrized by quantities that relate to the electron densities within the individual metal–ligand bonds. General chemical bonding principles that characterize conventional ligand-field analysis are used to interpret the parameter values of the present intensity analyses. Descriptions of the detailed nature of the coordination in the complexes arising from this intensity study agree in detail with those deriving from earlier ligand-field analyses of transition energies, paramagnetic susceptibilities, and ESR g values.

Introduction

The data base of ligand-field analysis for transition-metal and lanthanide complexes has traditionally comprised spectral transition energies together with paramagnetic susceptibilities and ESR g values. The sophistication of modern ligand-field analysis is such that we now expect to reproduce each of these properties, quantitatively within experimental error, for all mononuclear higher oxidation state (Werner-type) transition-metal complexes, regardless of coordination number, molecular geometry or symmetry, or of d^n or f^n configuration.[1] The greatest chemical transparency attaches to those ligand-field models with parameters that refer to local bonding features in molecules. The cellular ligand-field (CLF) model, like the molecular-orbital-based scheme of the angular overlap model (AOM) that preceded it, employs separate parameters for each ligand and for each local bonding mode (σ, π_x, π_y). The age-old chemical notion of the functional group is thus built into the best modern ligand-field schemes from the beginning.[1-4] It is just these structural features that endow

† No reprints are available from this laboratory.

(1) Gerloch, M. *Magnetism and Ligand-Field Analysis*; Cambridge University Press: Cambridge, England, 1983.

0020-1669/89/1328-2975$01.50/0